Molecular Cloning and Expression of a Functional Snake Venom Serine Proteinase, with Platelet Aggregating Activity, from the *Cerastes cerastes* Viper[†,‡]

Hafedh Dekhil,[§] Anne Wisner,[||] Naziha Marrakchi,[§] Mohamed El Ayeb,[§] Cassian Bon,[||] and Habib Karoui*[,§]

Laboratoire des Venins et Toxines, Institut Pasteur de Tunis, 13 place Pasteur, 1002 Tunis Belvédère, Tunisia, and Unité des venins, Institut Pasteur, 25 rue du Docteur Roux, 75724 Paris Cedex 15, France

Received May 14, 2003; Revised Manuscript Received July 2, 2003

ABSTRACT: The venoms of Viperidae snakes contain numerous serine proteinases that have been recognized to possess one or more of the essential activities of thrombin on fibrinogen and platelets. Among them, a platelet proaggregant protein, cerastocytin, has been isolated from the venom of the Tunisian viper *Cerastes cerastes*. Using the RACE-PCR technique, we isolated and identified the complete nucleotide sequence of a cDNA serine proteinase precursor. The recombinant protein was designated rCC-PPP (for *C. cerastes* platelet proaggregant protein), since its deduced amino acid sequence is more than 96% identical to the partial polypeptide sequences that have been determined for natural cerastocytin. The structure of the rCC-PPP cDNA is similar to that of snake venom serine proteinases. The expression of rCC-PPP in *Escherichia coli* system allowed, for the first time, the preparation and purification of an active protein from snake venom with platelet proaggregant and fibrinogenolytic activities. Purified rCC-PPP efficiently activates blood platelets at nanomolar (8 nM) concentrations, as do natural cerastocytin (5 nM) and thrombin (1 nM). It is able to clot purified fibrinogen and to hydrolyze α-chains. Thus, rCC-PPP could be therefore considered a cerastocytin isoform. By comparison with other snake venom serine proteinases, a Gly replaces the conserved Cys^{42}. This implies that rCC-PPP lacks the conserved Cys^{42}−Cys^{58} disulfide bridge. A structural analysis performed by molecular modeling indicated that the segment of residues Tyr^{67}−Arg^{80} of rCC-PPP corresponds to anion-binding exosite 1 of thrombin that is involved in its capacity to induce platelet aggregation. Furthermore, the surface of the rCC-PPP molecule is characterized by a hydrophobic pocket, comprising the 90 loop (Phe^{90}−Val^{99}), Tyr^{172}, and Trp^{215} residues, which might be involved in the fibrinogen clotting activity of rCC-PPP.

Snake venom glands contain a large variety of enzymes and other toxic polypeptides. These venom components are directly, or indirectly, involved in the various symptoms observed during envenomations. Thus, they are largely responsible for snakebite morbidity and mortality that represent a significant human, medical, and economic toll, particularly in the rural tropic (*1*). It is well-established that numerous snake venom components belong to the family of serine proteinases and that they act on different steps of the blood coagulation cascade. These serine proteinases are responsible for disorder in blood coagulation and hemorrhagic behavior of the prey (*2*). Up to now, venom serine proteinases were characterized mostly in the snake venoms of the Viperidae and Crotalidae families. Among the various serine proteinases from snake venom, some of them resemble thrombin in their ability to trigger the clotting of fibrinogen through fibrinopeptide release, while other ones lack fibrinogen clotting activity but can directly aggregate platelets in platelet-rich plasma and washed platelet suspensions (*3*). Several serine proteinases with platelet proaggregant activities were described, in particular, crotalocytin (*4*), MSP1[1] (*5*), thrombocytin (*6*), PA-BJ (*3*), and cerastocytin (*7*). In addition, platelet activation by PA-BJ and thrombocytin has been proven to be mediated through PAR 1 and PAR 4 (*8*), as in the case of thrombin effects on platelets. Further, it has been shown that PA-BJ and thrombocytin activate PAR 1, splitting its Arg^{41}−Ser^{42} peptide bond like α-thrombin (*8*).

Cerastocytin has been identified and purified from the venom of the desert viper *Cerastes cerastes*. Cerastocytin is a serine proteinase made of a single polypeptide chain of 38 kDa, which is a thrombin-like enzyme (*7*). Like thrombin, cerastocytin is a potent inducer of platelet aggregation, with a half-effective concentration of 2−5 nM, and its mechanism

[†] This work was supported by Secretariat d'Etat à la Recherche Scientifique et Technique PNM Grant P95/SP27GH and by Comité Mixte Franco-Tunisien pour la Coopération Universitaire Grant 96/F 09023.

[‡] The nucleotide sequence reported in this paper has been submitted to the EMBL Nucleotide Sequence Database as entry AJ553977.

* To whom correspondence should be addressed: Laboratoire des Venins et Toxines, Institut Pasteur de Tunis, 13 place Pasteur, 1002 Tunis Belvédère, Tunisia. Phone: 00 216 71 843 755 (ext. 420). Fax: 00 216 71 791 833. E-mail: habib.karoui@pasteur.rns.tn.

[§] Institut Pasteur de Tunis.

[||] Institut Pasteur.

[1] Abbreviations: cDNA, complementary deoxyribonucleic acid; HEPES, 4-(2-hydroxyethyl)-1-piperazineethanesulfonic acid; KN-BJ, kininogenase from *Bothrops jararaca*; MSP1, *moojeni* serine proteinase 1; mRNA, messenger RNA; PA-BJ, platelet aggregating enzyme from *Bothrops jararaca*; PAR, protein activator receptor of thrombin; PCR, polymerase chain reaction; RACE, rapid amplification of cDNA ends; rCC-PPP, recombinant *C. cerastes* platelet proaggregant protein; RT-PCR, reverse transcriptase PCR; SDS−PAGE, sodium dodecyl sulfate−polyacrylamide gel electrophoresis; TLf1, *Trimeresurus flavoviridis* serine proteinase 1; TSV-PA, *Trimeriserus stejnegeri* venom plasminogen activator.

10.1021/bi034790b CCC: $25.00
Published on Web 08/15/2003

of platelet activation appears to be similar to that of thrombin (*7*). However, the two enzymes have different sensitivities to selective inhibitors; for example, hirudin or the combination of antithrombin III and heparin inhibited platelet aggregation induced by thrombin but not the platelet aggregation induced by cerastocytin (*7*).

In this report, we describe the molecular cloning of a cDNA encoding a cerastocytin-like protein that has been successfully expressed in *Escherichia coli* and characterized as a recombinant and active protein. This is the first preparation of an active recombinant serine proteinase from snake venom that possesses platelet proaggregant and fibrinogenolytic activities. In addition, the biochemical characteristics, the enzymatic properties, and the structure−function relationships of this recombinant serine proteinase affecting hemostasis were investigated.

EXPERIMENTAL PROCEDURES

Materials. Venom was collected from mature *C. cerastes* snakes of both sexes in the Serpentarium of Institut Pasteur de Tunis. MonoS (HR 5/5) columns for fast performance liquid chromatography (FPLC) were from Pharmacia (Uppsala, Sweden). Chromogenic synthetic substrates H-D-Phe-Pip-Arg-*p*-nitroanilide (S-2238) and H-D-Val-Leu-Lys-*p*-nitroanilide (S-2251) were from Kabi-Vitrum (Stockholm, Sweden). All oligonucleotide primers were synthesized by Genset Laboratory (Paris, France).

Amplification of a cDNA Internal Fragment by PCR. On the basis of the determined N-terminal and internal polypeptide sequences of cerastocytin (*7*) and Marrakchi et al. (unpublished data), four oligonucleotide primers (S_1, P_2, P_{5r}, and P_{6r}) were designed for the amplification of a cDNA internal fragment by PCR, based on the analysis of genetic code usage for the published cDNA sequences, corresponding to venom proteinases batroxobin (*9*), ancrod (*10*), and TSV-PA (*11*). Primer S_1 (5′-GTCTTTGGAGGTGATGAATGT-3′) is oriented in the sense direction and corresponds to N-terminal residues 1−7 of cerastocytin. Primer P_2 (5′-ACTTTGATCAACAARGAATGGGT-3′) is oriented in the sense direction and corresponds to residues 26−37 of cerastocytin. Primer P_{5r} (5′-ACATGTATCTATGCCTC-CYTT-3′) is oriented in the antisense direction and corresponds to residues 173−180 of cerastocytin. Primer P_{6r} (5′-ATCCAGTVTGTATAATCGAAGACCTT-3′) is oriented in the antisense direction and corresponds to residues 214−222 of cerastocytin. Total RNA was prepared from *C. cerastes* venom glands according to the method of Chomezynski and Sacchi (*12*). Single-stranded cDNAs were prepared from the mRNAs contained in the total RNA preparation (5 μg) by reverse transcriptase (Life Technologies, Inc.), using oligo-d$(T)_{18}$ primers. A first amplification by PCR with the primers S_1 and P_{6r} was carried out using pfu polymerase (Stratagene), under the following conditions: a first denaturing step of 3 min at 94 °C followed by 30 cycles of 1 min at 94 °C, 1 min at 60 °C, and 1 min at 72 °C. A second internal amplification with P_2 and P_{5r} primers was carried out under the same conditions. From the sequences of the cDNA fragments obtained from the second PCR amplification, rCC-PPP specific primers were defined to be used in RACE-RT-PCR and designated P_9 (5′-ACTGTGTGAAA-GAGCTTACAATGATCT-3′), oriented in the sense direction, and P_{9r} (5′-AGATCATTGTAAGCTCTTTCACACAGT-3′), oriented in the antisense direction.

RACE-RT-PCR. Based on the very conserved sequences of the untranslated cDNA regions and signal peptides of TSV-PA (*11*), KN-BJ (*13*) and TLf1 (*14*) two oligonucleotide primers, PS (5′-ATGGTGCTGATCAGCGTGCTAGCAAGC-CTTCTG-3′), an oligonucleotide oriented in the sense direction that corresponds to the 33 first nucleotides of the signal peptide, and Ncr2 (5′-AACTGCCTGGGAATATAT-TCCACTGCAGTTGAA-3′), an oligonucleotide oriented in the antisense direction that corresponds to the sequence of the 3′-UTR. PS and Ncr2 were used in combination with P_9 and P_{9r} for 5′ and 3′ RACE-RT-PCR, performed essentially as described by Frohman (*15*). These amplifications allowed us to obtain the full-length cDNA sequence encoding rCC-PPP. In the case of 5′ RACE-RT-PCR amplification, the reverse transcription was performed by using primer P_{9r}. Then PCR amplification was carried out by using P_{9r} and PS. For the amplification of the 3′ end, the reverse transcription was performed by using oligonucleotide primer Ncr2. Then PCR amplification was carried out by using P_9 and Ncr2. The whole cDNA sequence was obtained by performing a third PCR overlapping the sequences of 3′ and 5′ RACE products using PS and Ncr2. The amplified product was first subcloned into the pGEM vector (Promega) and then sequenced on both strands. DNA sequencing was performed by the dideoxy terminal method using a T7 sequencing kit (LKB Pharmacia).

Construction of an rCC-PPP Expression Plasmid. The pET expression system (Novagen) was used for expression of rCC-PPP cDNA in *E. coli*. To subclone the rCC-PPP open reading frame from the cDNA into the pET-17b vector, a polymerase chain reaction was conducted with a forward primer, Penn, and a reverse primer, Petor. Primer Penn contains a *Hin*dIII site to facilitate subcloning (italic), the coding sequence for a tetrapeptide recognition site of factor Xa (bold), and five N-terminal residues of the rCC-PPP coding sequence (underlined) (5′-*AAGCTT***ATCGAAG-GTCGT**GTCATTGGAGGTGCT-3′). Primer Petor (5′-*CTCGAG***TCA**TTGGGGGCAAGTCG-3′) is an antisense oligonucleotide that contains an *Xho*I site to facilitate subcloning (italic), a stop codon (bold), and the coding sequence for the five C-terminal residues of a cerastocytin-like protein (underlined). The products, amplified with Penn and Petor, were first subcloned into the pGEM vector (Promega). After digestion with *Hin*dIII and *Xho*I, the recovered rCC-PPP open reading frame was ligated into the pET-17b vector at *Hin*dIII and *Xho*I sites, to generate the expression plasmid. The constructed plasmid was sequenced on both strands to ensure that the coding sequence of a cerastocytin-like protein was correct.

Expression and Folding of rCC-PPP. The expression and folding of rCC-PPP were performed according to the method of Zhang et al. (*16*), with some modifications. The sample was dialyzed, at 4 °C for 150 min, against 20 mM Tris-HCl (pH 8.0) containing 0.25 M NaCl, 2 mM EDTA, and 2 M urea. Bovine factor Xa was added at an enzyme:substrate ratio of 1:100, and digestion was conducted overnight at 37 °C. The protein was then fully denatured by incubation for 120 min at room temperature in 20 mM Tris-HCl (pH 9.5) containing 8 M urea, 2 mM EDTA, and 50 mM β-mercaptoethanol. The refolding was started by diluting the sample

50-fold in 20 mM Tris-HCl (pH 9.5) containing 2 mM EDTA. Then the refolding process was allowed to proceed at room temperature under constant agitation. It was monitored by assaying the amidolytic activity of rCC-PPP with the chromogenic substrate S-2238. When the enzyme activity reached a maximal level, usually after 30−48 h, the refolding mixture was stored at 4 °C for subsequent purification.

Purification of rCC-PPP. The purification of rCC-PPP was performed according to the last purification step used for natural cerastocytin from *C. cerastes* venom (*7*). Refolded rCC-PPP was first concentrated and dialyzed against 20 mM HEPES (pH 7.5). Then the sample was loaded on a FPLC MonoS HR5/5 column pre-equilibrated with dialysis buffer. Elution was carried out at a flow rate of 1 mL/min with a linear gradient from 0 to 1 M NaCl.

Measurement of Protein Concentrations. Protein concentrations were determined with the Bio-Rad protein assay.

SDS−Polyacrylamide Gel Electrophoresis. SDS−PAGE (20%) was performed with a Phast system apparatus (LKB Pharmacia). Samples were pretreated in 2% SDS and 5% β-mercaptoethanol at 100 °C for 5 min. Gels were stained with 0.1% Coomassie Brilliant Blue R in a methanol/acetic acid/water mixture (3:1:6) and destained in the same solution.

Chromogenic Assays and Kinetic Analysis. The amidolytic activity of the enzymes was measured with Beckman spectrophotometer in 1 cm path length plastic cuvettes as described by Zhang et al. (*11*). The concentration of chromogenic substrate S-2238 varied from 0.01 to 0.3 mM. The enzyme quantities were 0.3 μg.

Platelet Aggregation. Rabbit platelets were prepared from whole blood obtained from a 3−4 kg male (Hy/CR), with addition of 5 mM EDTA. Platelets were then separated from blood and washed as previously described by Ardlie et al. (*17*). Platelet aggregation was assessed by the turbidimetric method (*18*), using a chronolog aggregometer. Platelets (0.4 mL) were incubated with α-thrombin or rCC-PPP at 37 °C for 5 min.

Computer Analysis. Multiple alignments of protein sequence and nucleotide sequences were performed using Clustal X (*19*) and edited with GeneDoc (www.psc.edu/biomed/genedoc/). The sequence was also analyzed for the presence of mucin-type galactose N-acetyl-O-glycosylation and N-acetyl-N-glycosylation, using NetOGlyc 2.0 (www.cbs.dtu.dk/services).

Molecular Modeling and Structure Prediction. The protein sequences used and their accession numbers are as follows: rCC-PPP (this work), PA-BJ (SwissProt entry P81824), LM-TL (SwissProt entry P33589), TSV-PA (SwissProt entry Q91516), and human α-thrombin heavy chain (PDB entry 1PPB) (*20*). Molecular modeling was performed starting from the experimentally determined three-dimensional (3D) structure of TSV-PA resolved at 2.50 Å (PDB entry 1BQYA) (*21*) and used as a template. Automated homology models were generated by the Expert Protein Analysis System Proteomics server running at the Swiss Institute of Bioinformatics (Geneva, Switzerland), using SWISS-MODEL-ProModIII. The SWISS-PDB VIEWER software from the EXPASY server was used to visualize and compare the effect of the different substitutions on the structure and electrostatic potential of various molecular structures.

RESULTS

Molecular Cloning and Sequence Analysis. The purified cerastocytin from *C. cerastes* venom (*7*) was subjected to amino acid sequencing. The N-terminal amino acid sequence and the sequences of cerastocytin internal peptides generated by a trypsin treatment were obtained by Edman degradation. These polypeptide sequences are very similar to the sequence of snake venom serine proteinases such as PA-BJ, a platelet proaggregant from the venom of the snake *Bothrops jararaca* (*3*); LM-TL, a fibrinogenolytic enzyme from the venom of the snake *Lachesis muta* (*1*); and TSV-PA, a plasminogen activator from the venom of the snake *Trimeresurus stejnegeri* (*11*).

Specific oligonucleotide primers P_2 (in the sense direction and corresponding to cerastocytin N-terminal residues 26−37) and P_{5R} (in the antisense direction and corresponding to residues 173−180) were designed in regions of the polypeptide sequences that are very conserved among the above-mentioned snake venom serine proteinases. They were used to amplify by PCR partial cDNA sequences. Twenty-five different clones of ∼450 bases were sequenced, and their deduced amino acid sequences were compared to the partial polypeptide sequence determined for natural cerastocytin. The cDNA sequences that were most similar with that of natural cerastocytin were used to design specific cerastocytin primers, which were used to perform the 5′ and 3′ RACE-RT-PCR (*15*) that allowed us to obtain the complete cDNA sequence encoding a cerastocytin-like protein. These primers were designated P_9 and P_{9r}, and correspond to cerastocytin residues 132−161. In practice, the total RNA prepared from individual *C. cerastes* venom glands served as a template for the first-strand cDNA synthesis performed with Ncr_2 and P_{9r} primers. Then 3′ RACE-RT-PCR amplification was performed using an Ncr_2 cDNA preparation as a template with P_9 and Ncr_2 primers. Similarly, 5′ RACE-RT-PCR amplification was performed with the P_{9r} preparation as a template with PS and P_{9r} as specific primers. The whole cDNA sequence was obtained by performing a third PCR overlapping the sequences of the two 3′ and 5′ RACE products. This PCR-amplified product has the expected size for a cDNA encoding a cerastocytin-like protein. It was purified and cloned into the pGEM vector. A positive clone (0.87 kb insert) was identified and isolated. Both strands of the inserts were sequenced to confirm the primary structure of the cloned product. The complete nucleotide sequence of this cDNA clone and the deduced amino acid sequence are shown in Figure 1. The polypeptide sequence deduced from the cDNA clone was compared with the N-terminal amino acid sequence of natural cerastocytin, as well as with the amino acid sequences of internal peptides generated by trypsin digestion. Altogether, these polypeptide sequences represent almost 50% of the total sequence of cerastocytin. Interestingly, these alignments show a level of identity between the deduced sequence of rCC-PPP and that of natural cerastocytin of >96%. In fact, the cDNA-deduced amino acid sequence of rCC-PPP matched those determined for the sequenced fragments of natural cerastocytin apart from five differences: Asn^{35}, Cys^{58}, His^{72}, Arg^{80}, and Lys^{192} (α-chymotrypsinogen numbering scheme) (*21*) (Figure 2).

The cDNA structure of rCC-PPP is similar to that of other serine proteinases from snake venom. It contains a coding

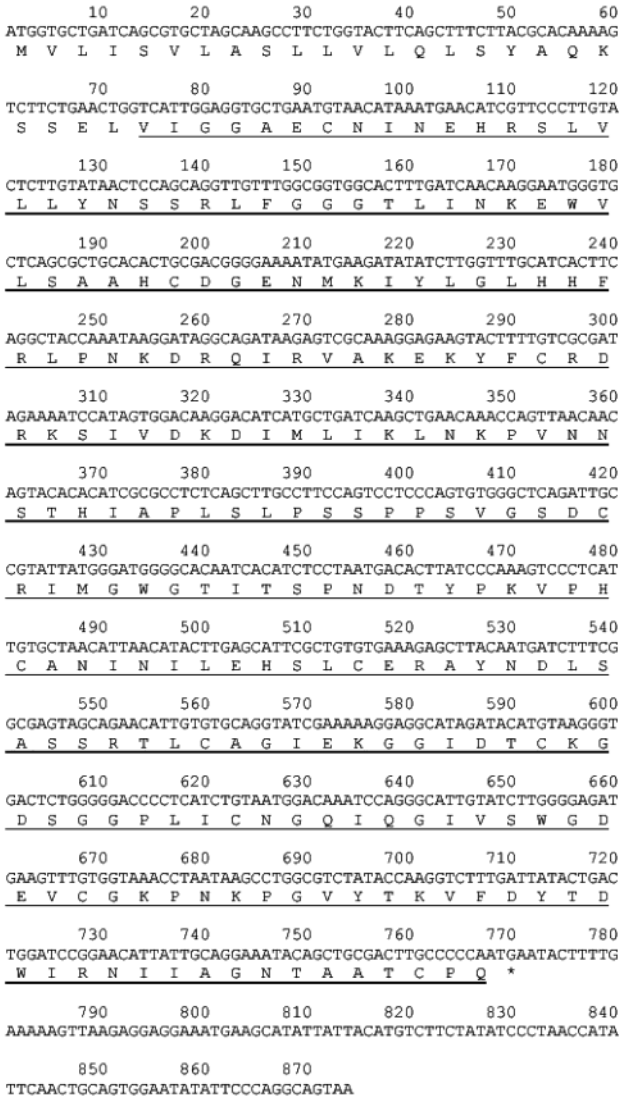

FIGURE 1: Nucleotide sequences of rCC-PPP cDNA and predicted amino acid sequence precursors. The nucleotide residues are numbered in the 5′ to 3′ direction. The numbering starts at the first amino acid of the signal peptide (methionine). The amino acid sequence of rCC-PPP is underlined. Potential glycosylation sites are indicated with bold characters.

region of 768 nucleotides that encode a polypeptide of 256 residues. The N-terminal residue valine of natural cerastocytin is preceded by a signal peptide of 24 amino acid residues, which are strictly identical to those reported for other snake venom serine proteinases. As already suggested (*3*, *11*, *13*, *14*), the signal peptide of cerastocytin consists of an amino-terminal hydrophobic prepeptide (18 amino acids) and a hydrophilic propeptide (six amino acids). The mature *C. cerastes* protein should have 232 residues, and its deduced molecular mass, before glycosylation, should be 25 386 Da. The difference noted with the apparent molecular mass of natural cerastocytin (38 kDa) is consistent with the presence of sugars. Accordingly, potential N-glycosylation sites, Asn-Xaa-Ser/Thr, are located at amino acid residues 35−37 and 113−116, and a potential O-glycosylation site is noted on Ser^{126}.

Sequence Analysis of rCC-PPP with Snake Venom Serine Proteinases. The amino acid sequence of mature rCC-PPP was compared with those of snake venom serine proteinases [PA-BJ, a platelet proaggregant enzyme from *B. jararaca* (*3*); LM-TL, a thrombin-like enzyme from *L. muta* (*1*); and TSV-PA, a plasminogen activator from *T. stejnegeri* (*11*)] as well as with that of human thrombin (*22*). Figure 2 shows a high level of sequence identity between snake venom serine proteinases (77% with TSV-PA and PA-BJ and 72% with LM-TL), while the similarity (44%) is less marked with human thrombin.

The sequence comparison allowed the identification of the catalytic triad of His^{57}, Asp^{102}, and Ser^{195} (α-chymotrypsinogen numbering scheme) (*21*). Furthermore, the analysis of structure motifs surrounding the residues of the active site and evolutionary markers led us to classify rCC-PPP in the S1 family of clan SA (*23*). A more detailed examination shows that in the sequence motif ^{54}SAAHC^{58}surrounding the catalytic His^{57}, Ser^{54} of rCC-PPP is substituted with Tyr in other serine proteinases (Figure 2). The sequence motif ^{102}DIML^{105} surrounding Asp^{102} is present in all snake venom serine proteinases, except in LM-TL, but replaced with the ^{102}DIAL^{105} motif in human thrombin. The motif surrounding Ser^{195} (^{193}GDSGGP^{198}) is conserved in rCC-PPP as in snake venom and mammalian serine proteinases. The evolutionary motif surrounding Ser^{214} (^{211}GIVSW^{215}) is conserved in rCC-PPP as in other enzymes, except in PA-BJ where Trp^{215} is substituted with Gly^{215}. Finally, the tetrad ^{225}(P/Y)GV(Y/F)^{228} is conserved in rCC-PPP and other snake venom serine proteinases, except in PA-BJ which has an Ala^{226}−Leu^{227} pair instead of a Gly^{226}−Val^{227} pair. Interestingly, rCC-PPP possesses a Pro^{225}, and this position has been shown to influence Na^+ binding near the primary specificity site and to contribute to its architecture. The presence of a Pro at position 225 abrogates the Na^+ binding (*24*).

Alignment of sequences revealed that rCC-PPP has an Asp^{189} residue in primary specificity site S1, Gly^{216} in site S3, and Gly^{226} in site S2, as in human thrombin and trypsin and as in numerous venom serine proteinases such as LM-TL. These characteristics allow easy access to the substrate side chain at the base of the catalytic site (*1*). On the other hand, the canonical Gly^{226} in the S2 site is substituted with a Ser in rCC-PPP, and with an Ala in PA-BJ. This probably reduces the substrate accessibility of these enzymes.

rCC-PPP contains 11 half-cystine residues. By homology with TSV-PA (*21*), 10 of them should form five of the intrachain disulfide bridges [Cys^{22}−Cys^{157}, Cys^{91}−Cys^{250}, Cys^{136}−Cys^{201}, Cys^{168}−Cys^{182}, and Cys^{191}−Cys^{220} (chymotrypsinogen numbering)] that are conserved in all snake venom serine proteinases. In rCC-PPP, Cys^{42} is substituted with a glycine residue, and consequently, the last disulfide bridge of snake venom serine proteinases (Cys^{42}−Cys^{58}) should not exist.

Expression of Recombinant rCC-PPP in E. coli. rCC-PPP has been overexpressed in *E. coli*, a major protein of 26 kDa being detected by SDS−PAGE in inclusion bodies (data not shown). Isolated inclusion bodies were dissolved in 8 M urea and then dialyzed against 20 mM Tris-HCl (pH 8) containing 2 mM EDTA and 2 M urea. The presence of urea at this concentration in dialysis buffer allowed us to avoid the problem of rCC-PPP aggregation. rCC-PPP was then cleaved by bovine factor Xa overnight at 37 °C, and the refolding of the mature protein was achieved at 30 °C by dilution in 20 mM Tris-HCl (pH 9.5) containing 2 mM EDTA. These

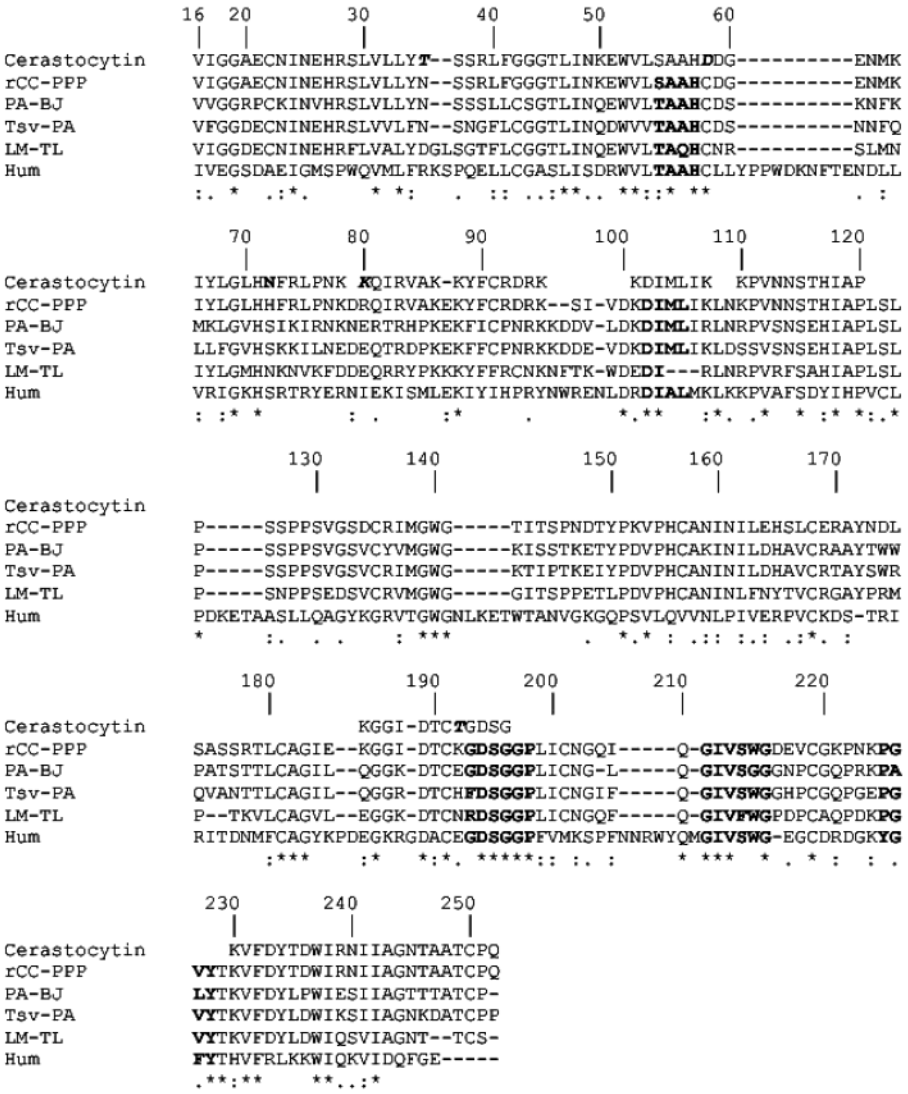

FIGURE 2: Multiple-amino acid sequence alignment of rCC-PPP (deduced from the nucleotide sequence) and natural cerastocytin determined by Edman degradation (ref *7* and unpublished data of N. Marrakchi et al.), PA-BJ (*3*), TSV-PA (*11*), LM-TL (*1*), and human thrombin (*22*). Differences are indicated with bold italic characters. The numbering refers to that of chymotrypsinogen (*21*). Gaps have been introduced to optimize the sequence similarities. The symbols indicate identical (∗) and similar residues (:) in all sequences. The motifs surrounding evolutionary markers and active site residues are given in bold characters.

refolding conditions allowed us to obtain an average of 1.5 mg of active protein from 10 mg of digested factor Xa protein. At this stage, active proteinase represents only 15% of the total proteins. Thus, active rCC-PPP was purified from misfolded and contaminant proteins by chromatography in a Mono S cation exchange column (Figure 3). Protein of peak 3, which is able to hydrolyze chromogenic substrates and which possesses platelet aggregating activity, represents purified rCC-PPP.

Analysis of Enzymatic and of Biological Activities of Recombinant and Purified rCC-PPP. The enzymatic activity of recombinant and purified rCC-PPP was examined by assessing the hydrolysis of synthetic and chromogenic substrates S-2238 and S-2251. A significant catalytic activity was noticed, and Michaelis constants K_m and k_{cat} were determined from Lineweaver−Burk plots. They are compared in Table 1 with those determined, under the same experimental conditions, for natural cerastocytin and rCC-PPP. As shown in Table 1, the values of the kinetic parameters of rCC-PPP and of natural cerastocytin are similar. In addition, the K_m values determined with S-2238 for rCC-PPP and cerastocytin are close to that reported for PA-BJ (320 μM) (*3*).

Like natural cerastocytin, purified rCC-PPP is a potent platelet proaggregant activator for washed rabbit platelets, as shown in Figure 4A. The proaggregant activity of purified rCC-PPP is dose-dependent, and a half-effective dose of 8 nM was determined (Figure 4B). This value is similar to the one measured for purified natural cerastocytin [5 nM (*7*)] and slightly higher than that calculated for thrombin [1 nM (*24*)].

Natural cerastocytin was shown to clot purified fibrinogen, hydrolyzing the α-chain only (*7*). Similarly, rCC-PPP is able to clot purified fibrinogen (not shown) and to hydrolyze the α-chain (Figure 5). The hydrolysis of the α-chain is complete within <0.5 h. However, Figure 5 further shows that rCC-PPP degrades also more slowly β- and γ-chains, since a significant hydrolysis of these chains can be noticed after incubation for only 3 h. So far, natural cerastocytin and rCC-PPP are serine proteinases that have both platelet aggregating

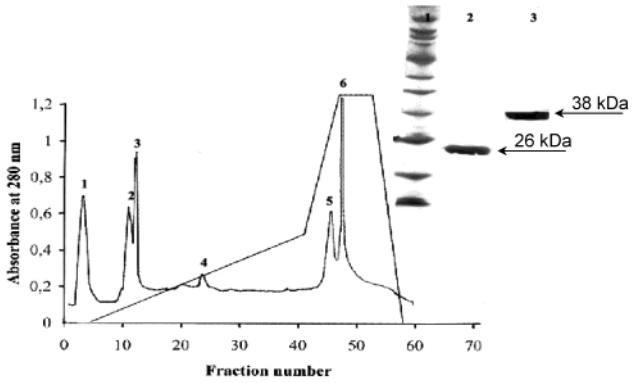

FIGURE 3: Purification of rCC-PPP. Refolded rCC-PPP was concentrated and then dialyzed against 20 mM HEPES (pH 7.5). The sample was loaded on a FPLC MonoS HR5/5 column. Elution was performed at a flow rate of 1 mL/min with a linear NaCl gradient (from 0 to 1 M). The aggregating activity was found in peak 3. The inset gives the results of SDS−PAGE (20% acrylamide) performed under reducing conditions: lane 1, molecular mass standard proteins; lane 2, purified rCC-PPP (i.e., fraction 3); and lane 3, natural cerastocytin.

Table 1: Comparison of Kinetic Parameters of the Enzymatic Activity of Natural Cerastocytin and rCC-PPP[a]

	natural cerastocytin			rCC-PPP		
	K_m (μM)	k_{cat} (min^{-1})	k_{cat}/K_m ($min^{-1}\,\mu M^{-1}$)	K_m (μM)	k_{cat} (min^{-1})	k_{cat}/K_m ($min^{-1}\,\mu M^{-1}$)
S-2238	309	857	2.7	366	558	1.52
S-2251	850	0.25	2.9×10^{-4}	666	5	0.75×10^{-4}

[a] The methods used for enzymatic assays and for the determination of the value of the kinetic parameters are described in Experimental Procedures. The data represent the mean of three independent determinations, which differed by 20%.

and fibrinogenolytic activities. Consequently, rCC-PPP has been considered a cerastocytin isoform both structurally and functionally.

Analysis of the 3D Structure rCC-PPP. The analysis of the multiple-sequence alignment of the venom serine proteinases indicates a remarkable conservation of their primary structure, of the elements implicated in the design of their secondary structure (α-helices, β-strands, and loops), and of their cysteine residues. Interestingly enough, the Cys^{42} that is conserved in all snake venom serine proteinases is replaced with a Gly. This was confirmed in natural cerastocytin N-terminal polypeptide sequencing. The undefined X residue previously reported (*7*) was confirmed to be a Gly. Consequently, the conserved $Cys^{42}-Cys^{58}$ disulfide bridge is present in neither rCC-PPP nor cerastocytin. Other residues at important positions for catalytic activity, namely, the residues of the catalytic triad and those of sites S1−S3, are also strictly conserved.

On the basis of these structural similarities and using the crystallographic data of TSV-PA (*21*), the theoretical 3D models were determined by molecular modeling for LM-TL, rCC-PPP proteins (Figure 6C,E), and PA-BJ (data not shown). This was achieved using SWISS-PDB VIEWER, as described in Experimental Procedures. Our model shows that the design of the 3D structure of rCC-PPP is maintained, and the amino acids involved in these serine proteinase structure motifs appear to be either conserved or replaced with similar residues. The hypothesized β/β hydrolase fold typical of several serine proteinases from the chymotrypsin family was conserved (Figure 6E). The arrangement of disulfide bonds of rCC-PPP is topologically equivalent to that of serine proteinases, except for the $Cys^{42}-Cys^{58}$ bond that is missing. Moreover, Gly^{42} is close to Cys^{58}, so the overall structure of rCC-PPP remains similar to that of other snake venom serine proteinases. The seven-residue C-terminal extension of rCC-PPP, which is highly conserved among serine proteinases, is well-defined in the structure (Figure 6E). The spatial arrangement observed in our model will ensure the formation of a disulfide bond between Cys^{91} and Cys^{250}, characteristic of venom serine proteinases, including TSV-PA (*21*) and LM-TL (*1*).

Proaggregant activity of thrombin is mainly attributed to the interaction of thrombin exosite 1 with the receptor PAR 1. This anion binding exosite is defined by the segment of residues $Arg^{67}-Ile^{80}$ (*25*). The comparison of the theoretical

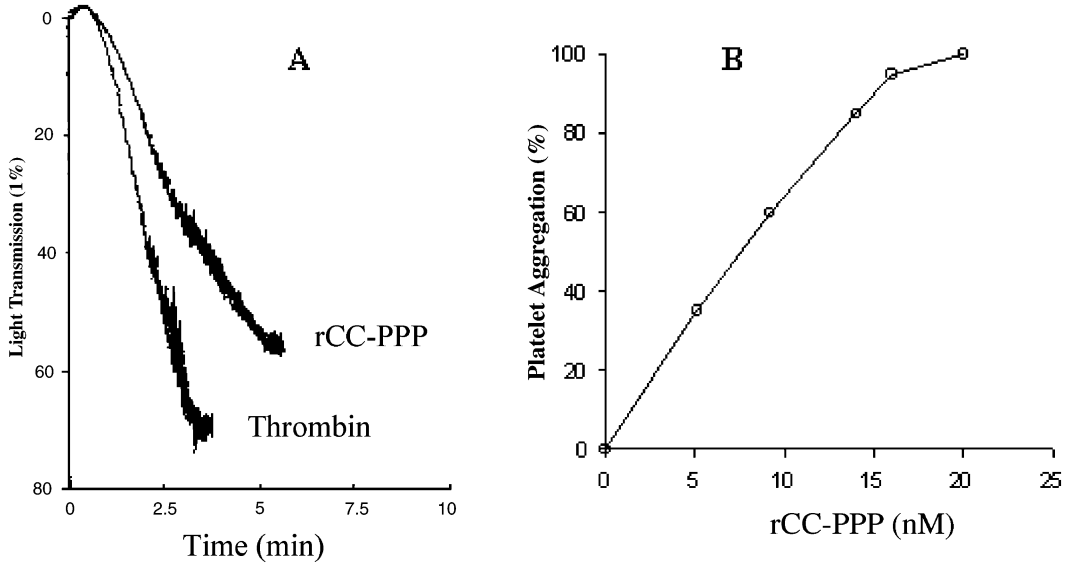

FIGURE 4: Platelet aggregation induced by rCC-PPP. (A) Platelet aggregation curve after addition of 1.8 μg/mL rCC-PPP or 0.25 μg/mL human thrombin. (B) Effect of rCC-PPP dose on platelet aggregation. The level of platelet aggregation measured 5 min after addition of the indicated concentration of rCC-PPP was expressed as the percentage of the maximal aggregation determined with α-thrombin.

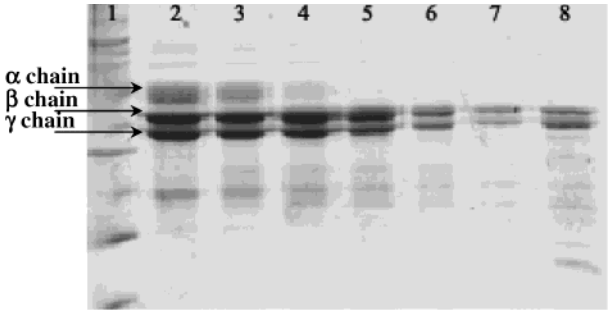

FIGURE 5: Hydrolysis of fibrinogen by rCC-PPP. Purified fibrinogen (1%) was incubated with purified rCC-PPP (1.5 μg/mL). Aliquots were removed at the indicated time and analyzed by SDS−PAGE (15%) under reducing conditions: lane 1, molecular mass standard proteins; and lanes 2−8, fibrinogen incubated with purified rCC-PPP for 0 min, 5 min, 30 min, 1 h, 3 h, 8 h, and 24 h, respectively.

3D models and the crystallographic structure of thrombin (*20*), especially at the level of Arg^{67}−Ile^{80}, indicates that this loop projects out of the molecular surface of thrombin (Figure 6A), LM-TL (Figure 6C), rCC-PPP (Figure 6E), and PA-BJ (data not shown), and forms a positively charged rim in platelet proaggregant proteins, but not in LM-TL. The various representations shown in Figure 6 reveal the differences in electric charges between the molecules in this area. The strong positive surface (in blue) of residues Tyr^{67}−Arg^{80} in rCC-PPP (Figure 6F) and Arg^{67}−Ile^{80} (Figure 6B) in thrombin is obvious, whereas LM-TL (in red) exhibits a mostly negative surface of residues Tyr^{67}−Glu^{80} (Figure 6D). In PA-BJ, the segment of residues Lys^{67}−Glu^{80} presents a strong positive surface (data not shown) as for rCC-PPP and thrombin.

The analysis of the 3D molecular model of the *L. muta* thrombin-like enzyme, which has been reported recently (*1*), has revealed a unique hydrophobic pocket (Phe^{95}−Trp^{99}, Tyr^{172}, Phe^{214}, and Trp^{215}) comparable to that found in the thrombin involved in the binding of fibrinopeptide A. The studies of Castro et al. revealed first that Arg^{16} of fibrinopeptide A is making a salt bridge with Asp^{189} of LM-TL and keeping it proximal to the catalytic triad. Second, as expected, Phe^{8}, which is believed to be critical for efficient thrombin-catalyzed proteolysis of fibrinogen, and Leu^{9} of fibrinopeptide A occupy the hydrophobic pocket of LM-TL in a manner similar to that of the thrombin (*1*). The aryl binding site is therefore similar in thrombin and LM-TL. The analysis of the 3D models shows that the hydrophobic amino acids involved in the interaction with fibrinogen are Leu^{99}, Ile^{174}, and Trp^{215} in α-thrombin (Figure 7A), Phe^{95}, Thr^{96}, Tyr^{172}, and Trp^{215} in LM-TL (Figure 7B), and Ile^{98}, Val^{99}, Tyr^{172}, and Trp^{215} in rCC-PPP (Figure 7C). The 90-loop (Phe^{90}−Val^{99}), Tyr^{172}, and Trp^{215} residues of rCC-PPP then form a hydrophobic pocket, and a similar structure exists in α-thrombin and LM-TL (Figure 7A,B). Therefore, the rCC-PPP hydrophobic pocket should be participating in the cleavage of fibrinogen as a consequence of accommodation of the apolar residues usually found in fibrinopeptide A (Phe^{8} and Leu^{9}) (*1*). More interesting is the Trp^{215} conserved in human α-thrombin and in venom serine proteinases rCC-PPP and LM-TL, pointing to the importance of this residue in fibrinogenolytic activity.

DISCUSSION

Several proteins, which share common properties with thrombin, have been purified to homogeneity from *C. cerastes* venom. They include cerastocytin (*7*) and cerastotin (*26*). These proteins are characterized by a marked platelet proaggregant action and a weak procoagulant activity. Nanomolar concentrations of cerastocytin induce aggregation of blood platelets (*7*). Studies of structure−function relationships of proaggregant protein and the analysis of their activities *in vivo* require large amounts of protein. To overcome this obstacle, we cloned and expressed, for the first time, a platelet proaggregant protein from snake venom.

In this report, we describe the construction of a cDNA encoding the precursor of a *C. cerastes* venom protein, by RACE-RT-PCR. This protein, whose amino acid sequence is more than 96% similar with the known polypeptide sequence of cerastocytin (Figure 2), is called rCC-PPP. The small differences in the amino acid sequence between rCC-PPP and cersatocytin might result from individual and/or geographical variations between the snake used for the collection of venom proteins and the venom glands. The deduced amino acid sequence of rCC-PPP contains two potential N-glycosylation sites and is between 66 and 81% similar with sequences of other venom serine proteinases. The similarity of rCC-PPP with venom and mammalian serine proteinases was further confirmed by the presence of the highly conserved amino acid residues, which form their catalytic triad of His^{57}, Asp^{102}, and Ser^{195} (chymotrypsinogen numbering) and their flanking sequences.

All the venom serine proteinases contain six well-conserved disulfide bridges, whereas rCC-PPP contains only 11 half-cystine residues, which probably form only five intrachain disulfide bridges. The missing bridge is the Cys^{42}−Cys^{58} bridge. In both PA-BJ and TSV-PA, the Cys^{42}−Cys^{58} disulfide bridges form with residues 40 and 41, the S1′ site (*21*). This cavity is rather open and exposed to the solvent; for rCC-PPP, the lack of this cystine bridge should keep this cavity more exposed.

The residue at position 193, which belongs to the S2′ subsite, plays a key role in the determination of the macromolecular specificity of serine proteinases. In TSV-PA, Phe^{193} is involved in the hydrolysis of plasminogen and in the reduced sensitivity of this enzyme to Kunitz-type inhibitors such as bovine pancreatic trypsin inhibitor (*21*, *27*). In LM-TL, this residue is an Arg^{193} and has been suggested by Castro et al. (*1*) to have a similar role in the fibrinogen clotting activity of this enzyme. However, this residue is Gly^{193} in rCC-PPP, as in thrombin and many other serine proteinases. Thus, the fibrinogen clotting activity does not seem to require an arginine residue at position 193, at least in thrombin and rCC-PPP. Our protein, like thrombin, might be then sensitive to Kunitz-type inhibitors.

Compared to other serine proteinases, rCC-PPP presents a two-residue deletion (Lys^{95} and Asp^{96}). This region, called the 99-loop, is located at the north of the active site and projects out of the molecular surface to form a highly charged rim (Lys^{94}-Lys^{95}-Asp^{96}-Asp^{97}-Glu^{98}-Val^{99}). A salt bridge, between Asp^{97} and Arg^{174}, stabilizes this loop and occludes the S4 binding pocket (*21*). In rCC-PPP, the 99-loop presents a deletion of Lys^{95} and Asp^{96} and the salt bridge that stabilizes the loop is missing since Asp^{97} and Arg^{174} are

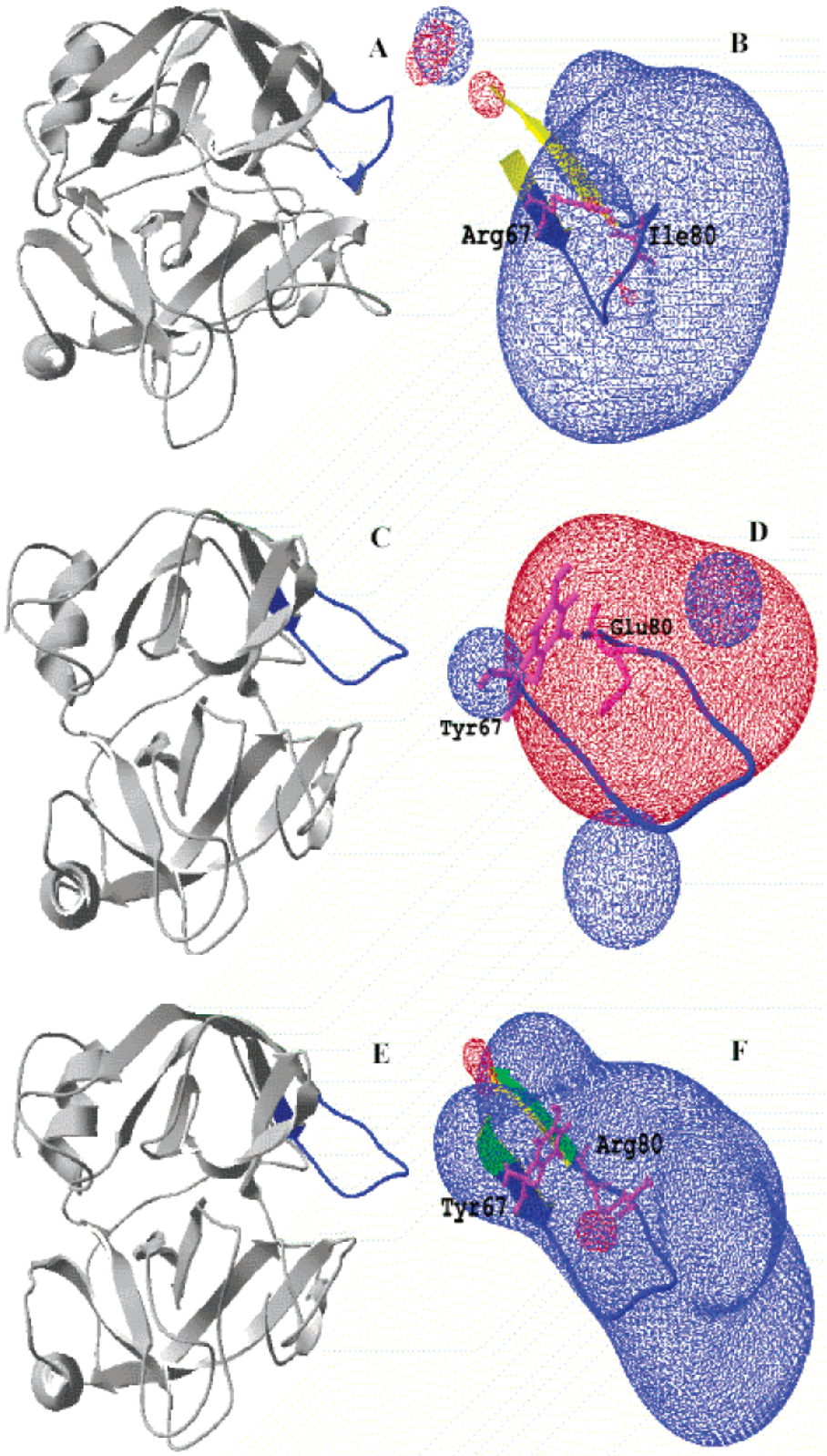

FIGURE 6: Structure and electrostatic potentials, respectively, of thrombin (A and B), LM-TL (C and D), and rCC-PPP (E and F). Molecular modeling was performed starting from the experimentally determined 3D structure of TSV-PA (PDB entry 1BQYA). The topology of rCC-PPP appears to be conserved, tough the $Cys^{42}-Cys^{58}$ bond is missing. Exosite 1 involved in the proaggregant activity of thrombin (A) and the equivalent segment in LM-TL (C) and rCC-PPP (E) are showen in blue. Electrostatic potentials of residues $Arg^{67}-Ile^{80}$ obtained with the SWISS-PDB VIEWER were computed from the human α-thrombin heavy chain (PDB entry 1PPB) and from theoretical structures of residues $Tyr^{67}-Glu^{80}$ of LM-TL and residues $Tyr^{67}-Arg^{80}$ of rCC-PPP. The different pictures reveal the differences in charge between the molecules, which can be observed as differences in color. Strong positive surfaces of the segment (in blue) are seen in rCC-PPP and thrombin, whereas LM-TL exhibits a mostly negative surface segment (in red).

substituted with Ser and Val, respectively. Therefore, in rCC-PPP, the 99-loop is held only by the disulfide bridge between Cys^{91} and Cys^{250} from the C-terminal extension that is strictly conserved among snake venom serine proteinases. The lack

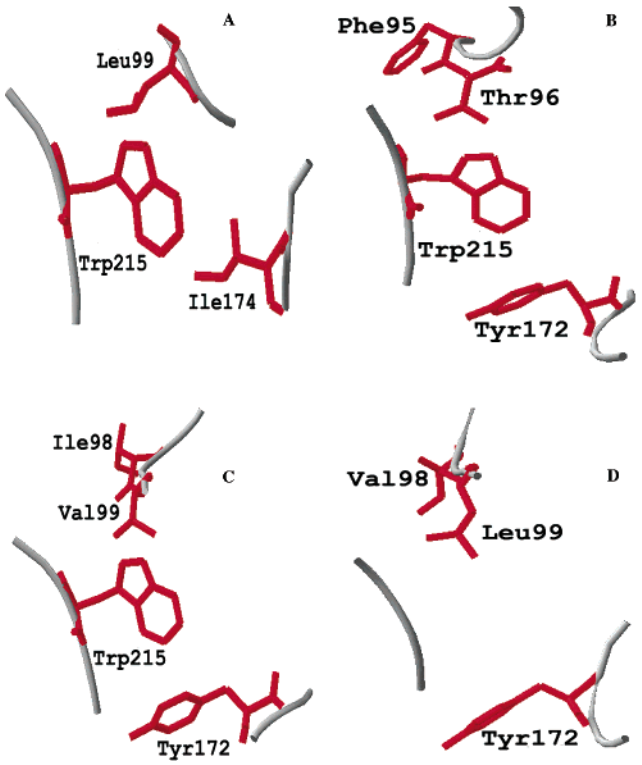

FIGURE 7: Details of the 3D structure of the putative fibrinogen binding site in α-thrombin (A), LM-TL (B), rCC-PPP (C), and PA-BJ (D). Hydrophobic amino acids involved in the interaction with fibrinogen are displayed: (A) α-thrombin formed by Leu^{99}, Ile^{174}, and Trp^{215}, (B) LM-TL formed by Phe^{95}, Thr^{96}, Tyr^{172}, and Trp^{215}, and (C) rCC-PPP formed by Ile^{98}, Val^{99}, Tyr^{172}, and Trp^{215}. These residues highlight part of the bioactive surface of proteins. (D) PA-BJ devoid of fibrinogenolytic activity is lacking amino acid Trp^{215}, which has been substituted with Gly^{215}, reducing the hydrophobicity of this pocket.

of these two residues leads to the shortening of this loop and may contribute to stabilization of the 99-loop.

Recently, Krem et al. have investigated the possible dominant role of the C-terminal sequence of serine proteinases. This sequence contains most of the structural determinants that are important for direct substrate recognition at the S1−S3 sites (*28*). rCC-PPP, TSV-PA, PA-BJ, and LM-TL present totally different biological activities, which could reinforce the link between structure−function relationship and this region for snake venom serine proteinases.

rCC-PPP was successfully expressed as a recombinant protein in an *E. coli* system. Very harsh conditions (2 M urea) were used to keep rCC-PPP in solution during factor Xa cleavage and refolding. Like natural cerastocytin isolated from *C. cerastes* venom, rCC-PPP hydrolyzes slowly the small synthetic peptide substrates such as S-2238 and S-2251. Like cerastocytin, it also clots purified fibrinogen and the slowly hydrolyzing α-chain. On the other hand, and like thrombin and cerastocytin, rCC-PPP aggregates efficiently blood platelets at nanomolar concentrations. Thus, rCC-PPP appears to be a cerastocytin isoform both functionally and structurally. Consequently, it should be considered as a thrombin-like snake venom enzyme that possesses a higher platelet aggregating activity than a fibrinogenolytic activity.

Actually, three different thrombin receptors were identified on human platelets, PAR 1, PAR 4, and GP Ib (*29*). It is assumed that thrombin activates platelet receptors PAR 1 and PAR 4. Recently, GP Ib was shown to be a functional thrombin receptor for platelet aggregation (*29*, *30*). Among serine proteinases from snake venoms, only PA-BJ and thrombocytin, from *B. jararaca* and *Bothrops atrox*, respectively, were shown to induce platelet aggregation through PAR 1 and PAR 4. This activation results from the interaction of the PA-BJ exosite with a lower affinity for thrombin receptor PAR 1 (*8*). This lower affinity is due to the low degree of similarity between the exosite domain of thrombin and the corresponding region of PA-BJ (*3*). The segment of residues Tyr^{67}−Arg^{80} of rCC-PPP, which corresponds to anion-binding exosite 1 of thrombin, contains an excess of basic amino acids over acidic ones (two Arg, one Lys, two His, and one Asp), like in the cases of PA-BJ (one Arg, three Lys, one His, and one Glu) and thrombin (four Arg, one Lys, one His, and two Glu), but not in that of snake venom proteinases without platelet aggregating activity. Since anion-binding exosite 1 of α-thrombin and of PA-BJ has been proven to be involved in their platelet aggregation activity (*25*), we propose that the corresponding segment of rCC-PPP is equivalent to exosite 1 of α-thrombin and has the same effect on platelet activation. Indeed, the theoretical 3D models indicate that residues Tyr^{67}−Arg^{80} in rCC-PPP and the equivalent fragment in PA-BJ make a solvent accessible and electropositive patch which might interact with the platelet receptor, as demonstrated for PA-BJ (*3*). As expected, the equivalent segment of LM-TL, which has no proaggregating activity on platelets, is electronegative. All these observations suggest that, like in α-thrombin, this positively charged segment is crucial for the platelet aggregation activity of rCC-PPP and PA-BJ. The preparation of mutants affecting this positively charged patch is being carried out in an effort to demonstrate unambiguously the implication of this segment in the interaction of rCC-PPP with the thrombin receptor, and consequently in its capacity to stimulate platelet aggregation. However, a new pathway mediated by GP Ib for α-thrombin platelet activation has been described recently by Soslau et al. (*29*) This hypothesis also needs to be investigated by site-directed mutagenesis in the case of rCC-PPP.

So far, snake venom serine proteinases affecting hemostasis, like human serine proteinases, contain 12 conserved cysteine residues paired in six disulfide bridges. Thrombin and PA-BJ are serine proteinases with six disulfide bridges and platelet aggregating activities. Interestingly, enough rCC-PPP with only 11 cysteine residues paired in five disulfide bridges is also a platelet aggregating serine proteinase; this missing disulfide bridge seems not to affect either the global structure of rCC-PPP or the platelet aggregating activity.

Thrombin acts on fibrinogen cleaving fibrinopeptides A and B using two distinct recognition sites (*31*−*33*). The site involved in binding of fibrinopeptide A in thrombin includes residues 97−99, Ile^{174}, and Trp^{215}. This region, called the aryl binding site, is conserved in thrombins from several species, apparently pointing to the importance of this site for fibrinogenolytic activity (*34*). As for native cerastocytin, rCC-PPP is able to clot fibrinogen α-chains, whereas, PA-BJ and thrombocytin induce platelet aggregation without clotting fibrinogen. When comparing rCC-PPP, LM-TL, and PA-BJ models with thrombin (Figure 7), we observe that the rCC-PPP surface has the same aryl binding site that thrombin and LM-TL do, while in PA-BJ, Trp^{215} is substi-

tuted with Gly. Because of its location, surrounding the S3 binding pocket, this substituted residue could be involved in the limited recognition and specific cleavage of fibrinogen. The lack of an aromatic ring of tryptophan in this environment reduces the hydrophobicity of this pocket. This effect suggests that Trp^{215} resides in the putative bioactive surface of PA-BJ upon fibrinogen. It is tempting to speculate that the aryl binding site of rCC-PPP is also involved in fibrinogen clotting activity. The importance of these regions on fibrinogen binding should be further investigated by mutational studies.

As suggested by Stubbs et al. (*33*), the thrombin and fibrinogen molecules complement each other over a large surface, with simultaneous interactions at the aryl binding site, the fibrinogen recognition exosite, and subsites S3−S3′. The S3′ site in thrombin formed by Glu^{39}, Leu^{41}, Cys^{42}−Cys^{58}, and Glu^{192} is implicated in the catalysis and release of fibrinopeptide α- and β-chains. As far as we know, the Cys^{42}−Cys^{58} disulfide bridge is only implicated in the S3′ site of thrombin; in this context, mutation of Glu^{39} to Lys (*35*) decreases the ability of thrombin to clot fibrinogen. In rCC-PPP, arginine at position 39 together with the missing Cys^{42}−Cys^{58} disulfide bridge may contribute to a release of fibrinopeptide α- and β-chains that is slower than that for the wild type. So far, this missing disulfide bridge does not interfere with the two main activities of rCC-PPP (i.e., fibrinogenolysis and platelet aggregation).

In conclusion, we propose that the effect of viper venom serine proteinase rCC-PPP on platelets and fibrinogen is mediated by the positively charged segment of residues Tyr^{67}−Arg^{80} and the aryl binding site, respectively. The missing disulfide bridge is not involved in the two main activities of rCC-PPP. The equivalent regions mediate the thrombin effects on platelets and fibrinogen.

ACKNOWLEDGMENT

We gratefully acknowledge Professor Koussay Dellagi for his constant interest in this work and for his helpful encouragement. We thank Dr. Ben Lasfar Zakaria, from the Serpentarium of Institut Pasteur de Tunis, for providing *C. cerastes* snakes and venoms.

REFERENCES

1. Castro, H. C., Silva, D. M., Craik, C., and Zingali, R. B. (2001) *Biochim. Biophys. Acta 1547*, 183−195.
2. Stocker, K. (1990) Snake venom proteins affecting hemostasis and fibrinolysis, in *Medical use of snake venom proteins* (Stocker, K., Ed.) pp 97−160, CRC Press, Boca Raton, FL.
3. Serrano, S. M., Mentele, R., Sampaio, C. A., and Fink, E. (1995) *Biochemistry 34*, 7186−7193.
4. Schmaier, A. H., and Colman, R. W. (1980) *Blood 56*, 1020−1028.
5. Serrano, S. M., Matos, M. F., Mandelbaum, F. R., and Sampaio, C. A. (1993) *Toxicon 31*, 471−481.
6. Kirby, E. P., Niewiarowski, S., Stocker, K., Kettner, C., Shaw, E., and Brudzynski, T. M. (1979) *Biochemistry 18*, 3564−3570.
7. Marrakchi, N., Zingali, R. B., Karoui, H., Bon, C., and El Ayeb, M. (1995) *Biochim. Biophys. Acta 1244*, 147−156.
8. Santos, A. B. F., Serrano, S. M. T., Kuliopulos, A., and Niewiarowski, S. (2000) *FEBS Lett. 477*, 199−202.
9. Itoh, N., Tanaka, N., Mihashi, S., and Yamashina, I. (1987) *J. Biol. Chem. 262*, 3132−3135.
10. Au, L. C., Lin, S. B., Chou, J. S., Teh, G. W., Chang, K. J., and Shih, C. M. (1993) *Biochem. J. 294*, 387−390.
11. Zhang, Y., Wisner, A., Xiong, Y., and Bon, C. (1995) *J. Biol. Chem. 270*, 10246−10255.
12. Chomczynski, P., and Sacchi, N. (1987) *Anal. Biochem. 162*, 156−159.
13. Serrano, S. M., Hagiwara, Y., Murayama, N., Higuchi, S., Mentele, R., Sampaio, C. A., Camargo, A. C., and Fink, E. (1998) *Eur. J. Biochem. 251*, 845−853.
14. Deshimaru, M., Ogawa, T., Nakashima, K., Nobuhisa, I., Chijiwa, T., Shimohigashi, Y., Fukumaki, Y., Niwa, M., Yamashina, I., Hattori, S., and Ohno, M. (1996) *FEBS Lett. 397*, 83−88.
15. Frohman, M. A. (1990) *Amplifications 5*, 11−15.
16. Zhang, Y., Wisner, A., Maroun, R. C., Choumet, V., Xiong, Y., and Bon, C. (1997) *J. Biol. Chem. 272*, 20531−20537.
17. Ardlie, N. G., Perry, D. W., Packham, M. A., and Mustard, J. F. (1971) *Proc. Soc. Exp. Biol. Med. 136*, 1021−1023.
18. Born, G. V. P., and Cross, M. J. (1963) *J. Physiol. 168*, 178−195.
19. Thompson, J. D., Gibson, T. J., Plewniak, F., Jeanmougin, F., and Higgins, D. G. (1997) *Nucleic Acids Res. 25*, 4876−4882.
20. Bode, W., Mayr, I., Baumann, U., Huber, R., Stone, S. R., and Hofsteenge, J. (1989) *EMBO J. 8*, 3467−3475.
21. Parry, M. A., Jacob, U., Huber, R., Wisner, A., Bon, C., and Bode, W. (1998) *Structure 6*, 1195−1206.
22. Degen, S. J., and Davie, E. W. (1987) *Biochemistry 26*, 6165−6177.
23. Krem, M. M., and Di Cera, E. (2001) *EMBO J. 20*, 3036−3045.
24. Dang, Q. D., and Di Cera, E. (1996) *Proc. Natl. Acad. Sci. U.S.A. 93*, 10653−10656.
25. Jakubowski, J. A., and Maraganone, J. M. (1990) *Blood 75*, 399−406.
26. Marrakchi, N., Barbouche, R., Guermazi, S., Karoui, H., Bon, C., and El Ayeb, M. (1997) *Eur. J. Biochem. 247*, 121−128.
27. Braud, S., Bon, C., and Wisner, A. (2000) *Biochimie 82*, 851−859.
28. Krem, M. M., Rose, T., and Di Cera, E. (1999) *J. Biol. Chem. 274*, 28063−28066.
29. Soslau, G., Class, R., Morgan, D. A., Foster, C., Lord, S. T., Marchese, P., and Ruggeri, Z. M. (2001) *J. Biol. Chem. 276*, 21173−21183.
30. Ramakrishnan, V., DeGuzman, F., Bao, M., Hall, S. W., Leung, L. L., and Phillips, D. R. (2001) *Proc. Natl. Acad. Sci. U.S.A. 98*, 1823−1828.
31. Bode, C., Baumann, H., von Hodenberg, E., Freitag, M., and Nordt, T. (1993) *Z. Kardiol. 82*, 125−128.
32. Di Cera, E., Dang, Q. D., and Ayala, Y. (1997) *Cell. Mol. Life Sci. 53*, 701−730.
33. Stubbs, M. T., Oschkinat, H., Mary, I., Huber, R., Angliker, H., Stone, S. R., and Bode, W. (1992) *Eur. J. Biochem. 206*, 187−195.
34. Banfield, D. K., and MacGillivray, R. T. A. (1992) *Proc. Natl. Acad. Sci. U.S.A. 89*, 2779−2783.
35. LeBonniec, B. F., MacGillivray, R. T., and Esmon, C. T. (1991) *J. Biol. Chem. 266*, 13796−13803.

BI034790B